

# Comparative Study of Influence of pH on Structural and Magnetic Properties of Ni-Zn Spinel Ferrite by Wet Chemical Method

Kakade GN and Gunjal RP

Department of Physics, R.B. Narayanrao Borawake, College, Shirampur, 413709 (M.S.) India  
Email: [genudaskakade@gmail.com](mailto:genudaskakade@gmail.com)

## Manuscript Details

Available online on <http://www.irjse.in>  
ISSN: 2322-0015

Editor: Dr. Arvind Chavhan

## Cite this article as:

Kakade GN and Gunjal RP. Comparative Study of Influence of pH on Structural and Magnetic Properties of Ni-Zn Spinel Ferrite by Wet Chemical Method, *Int. Res. Journal of Science & Engineering*, January 2018; Special Issue A2: 30-34.

© The Author(s). 2018 Open Access

This article is distributed under the terms of the Creative Commons Attribution 4.0 International License

(<http://creativecommons.org/licenses/by/4.0/>), which permits unrestricted use, distribution, and reproduction in any medium, provided you give appropriate credit to the original author(s) and the source, provide a link to the Creative Commons license, and indicate if changes were made.

## ABSTRACT

In this work we have synthesis the Ni-Zn ferrite nanoparticles having composition  $Ni_{0.65} Zn_{0.35} Fe_2O_4$  at two  $p^H$  values 7 and 8, synthesized by wet chemical sol-gel autocombution method using L-Ascorbic acid as chelating agent. The single phase cubic spinel structure was confirmed by X-ray diffraction studies. The surface morphological studies were carried out using scanning electron microscopy using JEOL JSM-6360 scanning electron microscopy (SEM). The effect of  $p^H$  values on structural properties of synthesized nanoparticles has been investigated. Lattice parameter (a) increases, X-ray density ( $d_x$ ) decreases, Unit cell volume (V) increases and Crystallite size (t) increases with increase in  $p^H$  value from 7 to 8. The grain size obtained from SEM images show decreasing trend with increasing pH Value.

**Keyword:** Ni-Zn spinel ferrite, sol-gel auto combustion technique, XRD, SEM.

## INTRODUCTION

Nano sized spinel ferrite particles, a kind of soft magnetic material with structural formula  $M-Fe_2O_4$  are one of the most attracting a novel class of magnetic material due to their interesting and most important properties, such as low melting point, high specific heating, low saturation magnetic moment and low magnetic transition temperature [1, 2]. Ferrites with electrical, dielectric, magnetic, optical, gas sensing etc. properties find numerous applications in variety of fields [3].

The important electrical as well as magnetic properties of spinel ferrite are sensitive to various factors viz. synthesis technique, variation in synthesis parameters in corporation with dopants at interstitial sites and nature and amount of dopant [4]. The most influencing synthesis parameter is  $p^H$  of solution. Many of the applications of spinel ferrites depend upon synthesis parameters such as  $p^H$ , fuel, sintering temperature, sintering time etc. ultimately the size of nanoparticle. The properties of spinel ferrites can also be improve by suitable dopants or cautions and by optimizing the various synthesis parameters like  $p^H$ , sintering temperature, sintering time, sintering atmosphere [5-7].

## METHODOLOGY

In the synthesis of Nickel -Zinc spinel ferrite AR grade with high purity (99.99 %) nitrates of metal ions (Nickel, Zinc and ferric) were used and L-Ascorbic acid was used as fuel. All as nitrates and L-Ascorbic acid as per calculation was taken and dissolved in minimum amount of double distilled water in separate beaker. The metal nitrate to fuel ratio was taken 1:3. All these solutions are mixed homogenously in single beaker by continuous stirring. Ammonia was added to adjust the  $p^H$  of value 7 and 8 of initial solution. This solution was evaporated at  $75^{\circ}C$  to get a dense sticky gel, then temperature was increased to  $110^{\circ}C$  for the dehydration process. The temperature was then increased rapidly and when it reached

approximately  $120^{\circ}C$  large of gases ( $CO_2$ ,  $H_2O$ , and  $N_2$ ) were liberated and dark brown power was produced through combustion process. The prepared power of Ni-Zn spinel ferrite is sintered at  $500^{\circ}C$  for 6 h and various properties of Ni-Zn ferrite were studied.

## RESULT AND DISCUSSION

### Structural characterization:

Phase formation of the cubic spinel structure samples was examined by X-ray diffraction (XRD) pattern obtained using Rigaku Corporation, Japan diffractometer at room temperature. The pattern was recorded using Cu-K $\alpha$  radiation ( $\lambda=1.54182 \text{ \AA}$ ) in the  $2\theta$  range  $20^{\circ} - 80^{\circ}$  with step size  $0.02^{\circ}$  and time/step 2 s. Structural information such as the present phases, lattice parameter and crystalline size can be extracted from the samples diffraction pattern

### X-ray diffraction study:

Fig.1 (a) and (b) shows the x-ray diffraction pattern of Ni-Zn samples synthesized at  $p^H=7$  and  $p^H=8$ . X-ray diffraction analysis revealed that all the diffraction peaks seen in the XRD pattern well match with the standard pattern of pure nickel ferrite. The analysis of XRD pattern revealed the formation of single phase cubic spinel structure. The peaks of the XRD pattern corresponds to (220), (311), (222), (400), (422), (511) and (440) planes. The width of diffraction maxima peaks of planes (311) reduced and intensity of peaks increased as the  $p^H$  value increases.

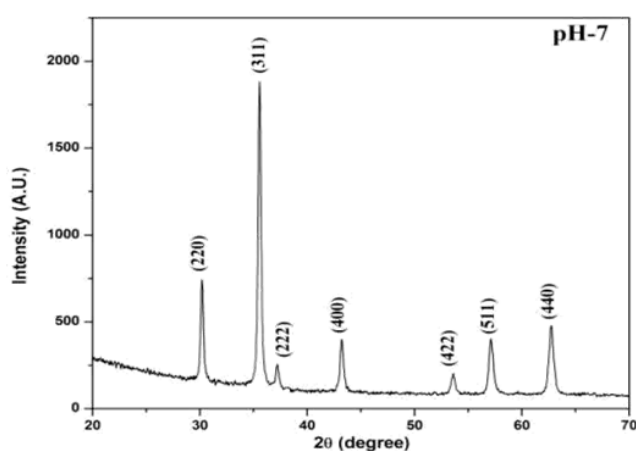
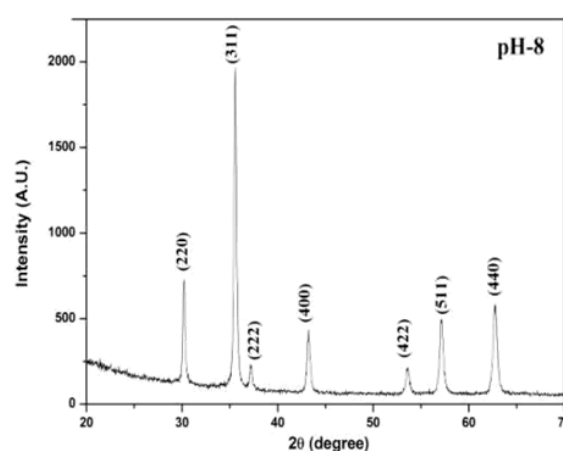


Fig.1 (a) x-ray diffraction pattern of  $Ni_{0.65}Zn_{0.35}Fe_2O_4$  nanoparticles for  $p^H=7$



(b) x-ray diffraction pattern of  $Ni_{0.65}Zn_{0.35}Fe_2O_4$  nanoparticles for  $p^H=8$

**Table 3.1 (a):** Miller indices (h k l), Bragg's angle ( $\theta$ ), Interplanar spacing (d), Intensity (I) and Relative intensity ratio (I/I<sub>0</sub>) of Ni<sub>0.65</sub>Zn<sub>0.35</sub>Fe<sub>2</sub>O<sub>4</sub> nanoparticles (pH- 7)

(h k l)	2 $\theta$ (degree)	$\theta$ (degree)	Sin ( $\theta$ )	Sin ( $\theta$ )/ $\lambda$	d (Å)	I (a.u)	I/I <sub>0</sub>
(220)	30.191	15.0955	0.2604	0.1690	2.9571	782.7	40
(311)	35.587	17.7935	0.3056	0.1984	2.5201	1933.4	100
(222)	37.257	18.6285	0.3194	0.2073	2.4109	277.5	14
(400)	43.227	21.6135	0.3683	0.2391	2.0907	425.0	22
(422)	53.601	26.8005	0.4509	0.2927	1.7080	222.8	12
(511)	57.116	28.5580	0.4780	0.3103	1.6109	434.3	22
(440)	62.699	31.3495	0.5203	0.3377	1.4802	512.5	27

**Table 3.1 (b):** Miller indices (h k l), Bragg's angle ( $\theta$ ), Interplanar spacing (d), Intensity(I) and Relative intensity ratio (I/I<sub>0</sub>) of Ni<sub>0.65</sub>Zn<sub>0.35</sub>Fe<sub>2</sub>O<sub>4</sub> nanoparticles (pH-8).

(h k l)	2 $\theta$ (degree)	$\theta$ (degree)	Sin ( $\theta$ )	Sin ( $\theta$ )/ $\lambda$	d (Å)	I (a.u)	I/I <sub>0</sub>
(220)	30.186	15.0930	0.2604	0.1690	2.95830	738.0	37
(311)	35.576	17.7880	0.3055	0.1983	2.52145	1977.3	100
(222)	37.175	18.5875	0.3188	0.2069	2.41658	253.8	13
(400)	43.214	21.6070	0.3682	0.2390	2.09183	450.6	23
(422)	53.559	26.7795	0.4506	0.2925	1.70964	210.2	11
(511)	57.084	28.5420	0.4778	0.3101	1.61216	520.6	26
(440)	62.764	31.3820	0.5207	0.3380	1.47923	608.5	31

**Table 3.2:** Lattice parameter (a), X-ray density (d<sub>x</sub>), Unit cell volume (V) and Crystallitesize (t) of Ni<sub>0.65</sub>Zn<sub>0.35</sub>Fe<sub>2</sub>O<sub>4</sub> nanoparticles (pH-7, 8)

'pH'	a	d <sub>x</sub>	V	Crystallite size
maintain at	(Å)	(gm/cm <sup>3</sup> )	(Å <sup>3</sup> )	(t)
pH-7	8.3640	5.3748	585.557	22
pH-8	8.3678	5.3671	586.334	24

**Table 3.3:** Hopping length (L<sub>A</sub>, L<sub>B</sub>), Tetrahedral bond (d<sub>AX</sub>), Octahedral bond (d<sub>BX</sub>), Tetraedge (d<sub>AXE</sub>) and Octa edge (d<sub>BXE</sub>) of Ni<sub>0.65</sub>Zn<sub>0.35</sub>Fe<sub>2</sub>O<sub>4</sub> nanoparticles (pH-7, 8).

'pH'	L <sub>A</sub>	L <sub>B</sub>	d <sub>AX</sub>	d <sub>BX</sub>	d <sub>AXE</sub>	d <sub>BXE</sub>	
Maintain at	(Å)	(Å)	(Å)	(Å)	(Å)	Shared	Unshared
pH-7	3.6217	2.9571	1.8978	2.0420	3.0911	2.8152	2.9588
pH-8	3.6235	2.9585	1.8987	2.0430	3.1005	2.8165	2.9602

Table 3.1(a) and (b) gives the miller indices (hkl), Bragg's angle ( $2\theta$ ) along with their corresponding interplanar spacing (d) values, intensity and relative intensity ratio of the Ni-Zn ferrite with varying pH values. It is seen that the interplanar spacing (d) values shows gradual decrease with increasing Bragg's angle. The intensity of (311) plane is more as compared to other planes. The lattice constant value

'a' (Å) of Ni<sub>0.65</sub>Zn<sub>0.35</sub>Fe<sub>2</sub>O<sub>4</sub> nanoparticles synthesized at different pH was determined by using the relation [9]. The obtained values of the lattice constant (a) are tabulated in Table 3.2. There is slight changes were observed for lattice constant 'a' which could be associated with the pH solution. The results presented in Table 4.2 show that the lattice parameters a, b and c agree with the equation a = b = c, indicating that the prepared sample belongs to cubic lattice. The average

crystallite size of  $\text{Ni}_{0.65}\text{Zn}_{0.35}\text{Fe}_2\text{O}_4$  nanoparticles synthesized at two pH value (pH-7,8) was determined using the relation [10].

The obtained values of the crystallite size are tabulated in Table 3.2. Using the Scherer's formula, the variations of full-width at half maximum (FWHM) at different XRD peaks indicated that the average crystallite size of the nanoparticles were about 22, 24 nm corresponding to the pH of 7, 8 respectively. The average crystallite size is increased as the pH increases. Due to the rapid combustion rate and high flame temperature with increasing pH, higher pH produces larger crystallite size and good crystallinity. It has been experimentally observed by some researchers that nanocrystalline powders are quite susceptible to the formation of inter-particle London-van der Waals bonds either in the wet or in the dry state due to their very fine particle size [11]. The X-ray density ( $d_x$ ) of  $\text{Ni}_{0.65}\text{Zn}_{0.35}\text{Fe}_2\text{O}_4$  nanoparticles synthesized at two pH value (pH -7, 8) was calculated by using the relation [8, 12].

The X-ray density depends on the molecular weights of the samples and lattice constants. The X-ray density values are tabulated in Table 4.2; the obtained values of X-ray density are in reported range, which are depends on lattice constant, therefore same nature of lattice constant observed in the X-ray density value with increase pH of sample. The value of volume of unit cell value determined from cube of lattice constant, which indicate that the volume of the unit cell depends on the lattice constant, therefore same nature of lattice constant observed in the volume of unit cell values with increase pH of sample.

Various other structural parameters like hopping lengths ( $L_A, L_B$ ), tetrahedral bond length ( $d_{AX}$ ), octahedral bond length ( $d_{BX}$ ), tetra edge ( $d_{AXE}$ ) and octa edge ( $d_{BXE}$ ) were evaluated from relation for two pH value [13, 14]. Using the values of the lattice constant ( $a$ ), the various other structural parameters like hopping lengths ( $L_A, L_B$ ), tetrahedral bond length ( $d_{AX}$ ), octahedral bond length ( $d_{BX}$ ), tetra edge ( $d_{AXE}$ ) and octa edge ( $d_{BXE}$ ) were evaluated from XRD data for different pH value and indexed in Table 3.3.

The obtained structural parameters are depends on lattice constant values, there were no increasing or

decreasing trend observed in the hopping lengths ( $L_A, L_B$ ), tetrahedral bond length ( $d_{AX}$ ), octahedral bond length ( $d_{BX}$ ), tetra edge ( $d_{AXE}$ ) and octa edge ( $d_{BXE}$ ) values with increasing pH value of Ni-Zn sample.

The tetrahedral A-site ionic radii can be calculated using the value of lattice constant ' $a$ ' and oxygen positional parameter ' $u$ ' ( $u = 0.381\text{\AA}$ ) as:

$$r_A = \left(u - \frac{1}{4}\right) a \sqrt{3} - r \left(\frac{2}{o}\right)^0 A$$

where, ' $r_A$ ' represents radius of tetrahedral (A) site cation, ' $u$ ' oxygen positional parameter, ' $O$ ' represents radius of oxygen anions. The octahedral B-site ionic radii can be calculated using the equation:

$$r_B = \left(\frac{5}{8} - u\right) a - r \left(\frac{2}{o}\right)^0 A.$$

Where,  $r_B$  represents radius of octahedral [B] site cation.

**Table 3.4:** Ionic radii ( $r_A, r_B$ ) of  $\text{Ni}_{0.65}\text{Zn}_{0.35}\text{Fe}_2\text{O}_4$  nanoparticles (pH-7, 8).

'pH' Maintain at	$r_A(\text{\AA})$	$r_B(\text{\AA})$
pH-7	0.5778	0.7208
pH-8	0.5787	0.7218

The values of tetrahedral (A-site) and octahedral [B-site] of ionic radius are given in Table 4.4. The values of tetrahedral (A-site) and octahedral [B-site] value depends on the values of lattice constant, therefore, it is found that obtained values tetrahedral (A-site) and octahedral [B-site] are in reported range. There are no more changes observed in tetrahedral and octahedral ionic radii values with increasing pH of sample [15, 16].

## CONCLUSION

Nanocrystalline Ni-Zn ferrite has been synthesized at different pH via Sol-gel auto combustion method, which is characterized on nanosized shape etc by X-Ray diffraction. The particle size is in the range of 22-24nm. The particle size increases with increase in pH value. The prepared Ni-Zn samples annealed at

temperature 500 °C for 2 hr is formed a good crystalline cubic phase spinel structure. The grain size is in the range of 78-89 nm for two pH values. With increase in pH from 7 to 8 the grain size decreases. The surface morphology of the prepared samples is strongly influenced by pH. The grain size obtained from SEM images show decreasing trend with increasing pH.

### Acknowledgement

The authors are very much thankful to Dr.K.M. Jadhav, Professor, Department of Physics Dr. Babasaheb Ambedkar Marathwada University, Aurangabad (M.S.),India for their fruitful guidance and for providing laboratory facilities.

**Conflicts of interest:** The authors stated that no conflicts of interest.

### REFERENCES

- Lu AH, Salabas EeL, Schüth F. Magnetic nanoparticles: synthesis, protection, functionalization, and application, *Angewandte Chemie International Edition*, 2007; 46; 1222-1244.
- Richerson DW. Modern ceramic engineering: properties, processing, and use in design, CRC press, 2005.
- Mathew DS, Juang RS. An overview of the structure and magnetism of spinel ferrite nanoparticles and their synthesis in microemulsions, *Chemical Engineering Journal*, 129 (2007) 51-65.
- Goldman A. Modern ferrite technology, Springer Science & Business Media, 2006.
- Teja AS, Koh PY. Synthesis, properties, and applications of magnetic iron oxide nanoparticles, *Progress in crystal growth and characterization of materials*, 55 (2009) 22-45.
- Rath C, Anand S, Das R, Sahu K, Kulkarni S, Date S, Mishra N. Dependence on cation distribution of particle size, lattice parameter, and magnetic properties in nanosize Mn-Zn ferrite, *Journal of Applied Physics*, 91 (2002) 2211-2215.
- Upadhyay C, Mishra D, Verma H, Anand S, Das R. Effect of preparation conditions on formation of nanophase Ni-Zn ferrites through hydrothermal technique, *Journal of Magnetism and Magnetic Materials*, 260 (2003) 188-194.
- Gul I, Ahmed W, Maqsood A. Electrical and magnetic characterization of nanocrystalline Ni-Zn ferrite synthesis by co-precipitation route, *Journal of Magnetism and Magnetic Materials*, 320 (2008) 270-275.
- Khirade PP, Birajdar SD, Humbe AV, Jadhav K. Structural, electrical and dielectrical property investigations of Fe-doped BaZrO<sub>3</sub> nanoceramics, *Journal of Electronic Materials*, 45 (2016) 3227-3235.
- Rajendran M, Pullar R, Bhattacharya A, Das D, Chintalapudi S, Majumdar C. Magnetic properties of nanocrystalline CoFe<sub>2</sub>O<sub>4</sub> powders prepared at room temperature: variation with crystallite size, *Journal of Magnetism and Magnetic Materials*, 232 (2001) 71-83.
- Hamaker H. The London-van der Waals attraction between spherical particles, *physica*, 4 (1937) 1058-1072.
- Kambale R, Shaikh P, Kamble S, Kolekar Y. Effect of cobalt substitution on structural, magnetic and electric properties of nickel ferrite, *Journal of Alloys and Compounds*, 478 (2009) 599-603. Vinayak V, Khirade PP, Birajdar SD, Gaikwad P, Shinde N, Jadhav K. Low temperature synthesis of magnesium doped cobalt ferrite nanoparticles and their structural properties, *Int. Adv. Res. J. Sci. Eng. Technol.*, 2 (2015) 55-58.
- Sindhu S, Birajdar D. Structural and magnetic characterization of Co<sup>2+</sup> substituted nano structured Copper-Zinc spinel ferrite, *IOSR Journal of Applied Physics*, 3 (2013) 33-41.
- El-Sayed A. Influence of zinc content on some properties of Ni-Zn ferrites, *Ceramics International*, 28 (2002) 363-367.
- Priyadharsini P, Pradeep A, Rao PS, Chandrasekaran G. Structural, spectroscopic and magnetic study of nanocrystalline Ni-Zn ferrites, *Materials Chemistry and Physics*, 116 (2009) 207-213.
- Janghorban K, Shokrollahi H. Influence of V<sub>2</sub>O<sub>5</sub> addition on the grain growth and magnetic properties of Mn-Zn high permeability ferrites, *Journal of magnetism and magnetic materials*, 308 (2007) 238-242.
- Thorvaldsen A. The intercept method – 2. Determination of spatial grain size, *Acta Materialia*, 45 (1997) 595-600.

© 2018 | Published by IRJSE

### Submit your manuscript to a IRJSE journal and benefit from:

- ✓ Convenient online submission
- ✓ Rigorous peer review
- ✓ Immediate publication on acceptance
- ✓ Open access: articles freely available online
- ✓ High visibility within the field

Email your next manuscript to IRJSE  
: editorirjse@gmail.com